Available online at www.sciencedirect.com
SCIENCE DIRECT®
Journal of Power Sources 122 (2003) 111–121
JOURNAL OF POWER SOURCES
www.elsevier.com/locate/jpowsour

Chemical storage of hydrogen by modified iron oxides

K. Otsuka*, T. Kaburagi, C. Yamada, S. Takenaka

Department of Applied Chemistry, Graduate School of Science and Engineering, Tokyo Institute of Technology, Ookayama, Meguro-ku, Tokyo 152-8552, Japan

Received 18 November 2002; accepted 14 February 2003

Abstract

Pure hydrogen may be supplied directly to polymer electrolyte fuel cell (PEFC) through the decomposition of water by reduced iron oxide at low temperatures <573 K. Effects of various metal additives in the reduced iron oxide on the production of hydrogen from water have been examined at a temperature range 373–873 K. The decomposition of water is caused by the oxidation of iron with water ($3Fe + 4H_2O \rightarrow Fe_3O_4 + 4H_2$). Among 26 metal elements examined as additives, Al, Mo and Ce were favorable ones for preserving the Fe/Fe_3O_4 sample from decaying its reactivity by repeated cycles. The decomposition of water was most repetitive for the reduced iron oxide added with Mo. The addition of Rh or Ir enhanced the rate of H_2O decomposition remarkably at <573 K. However, these noble metals could not suppress the sintering of the host iron or iron oxide. Co-addition of Rh and Mo, Zr, Al or Ga to the reduced iron oxide accelerated remarkably the decomposition of water at 473 K. It is suggested that Rh metal would catalyze the dissociation of H_2O at low temperature while the compound oxides formed between iron and additives mitigate the coagulation of iron and iron oxide particles during repeated reaction cycles.

Keywords: Chemical storage of hydrogen; Water decomposition; Redox of iron; Cooperative effect of Rh and Mo

1. Introduction

Hydrogen fuel cells are environmentally benign and highly efficient electrochemical systems converting the chemical energy of hydrogen directly into electricity. Therefore, the use of hydrogen in fuel cell vehicles and stationary fuel cell equipments is expected to increase dramatically in the near future. However, for a widespread use of hydrogen for fuel cells, well-ordered infrastructures will be required to transport and distribute hydrogen as well as to store it to match time and space between the production and end use. One of the major obstacles to the use of hydrogen as energy carrier is the lack of safe, efficient and low cost storage systems suitable for the various stationary and mobile applications.

Various methods are currently proposed and being developed for the direct or indirect storage of hydrogen. Hydrogen can be stored physically by changing its phase depending on temperature and pressure, or chemically in various solid and liquid compounds such as metal hydrides, hydrogen absorbing alloys, carbon nanotubes, boron hydrides and hydrocarbons. The choice of hydrogen storage system should be determined by taking into account various criteria at the present stage of related technologies. The criteria would be based on the transport and distribution infrastructure, handling safety, cycle life, safety in use, environmental impact of the storage material, and on the economics. The storage of hydrogen on polymer electrolyte fuel cell (PEFC) vehicles, one of the most challenging and competitive technology, requires high hydrogen density, nontoxic, safe handling, no explosion at car collision, short refueling time and low cost.

On the bases of these backgrounds, we have proposed a simple, safe and environmentally benign technology for the storage, transport and supply of hydrogen to PEFC vehicles [1]. The technology is based on a very simple redox reaction of magnetite (Eq. (1)).

$$Fe_3O_4 + 4H_2 \leftrightarrow 3Fe + 4H_2O \quad (1)$$

The principle of the technology is analogous to the old steam iron process which was extensively studied by the group of Institute of Gas Technology [2,3] for the production of hydrogen rich fuel gas at high temperatures >800 °C and pressures >70 bar by using a gas mixture of CO, CO_2 and H_2 from coal and biomass for the reduction of iron ores.

Our technology stands on the premise that hydrogen can be provided cheaply from natural gas, LPG or gasoline by steam reforming, partial oxidation or by direct cracking at

* Corresponding author. Tel.: +81-3-5734-2143; fax: +81-3-5734-2879.
E-mail address: kotsuka@o.cc.titech.ac.jp (K. Otsuka).

0378-7753/03/$ – see front matter © 2003 Elsevier Science B.V. All rights reserved.
doi:10.1016/S0378-7753(03)00398-7

suburban industries and at residential gas stations. Fe_3O_4 must first be reduced with hydrogen (Eq. (2)) at suburban H_2 production plants or at residential gas stations.

Step 1: chemical H_2 storage.

$$Fe_3O_4 + 4H_2 \rightarrow 3Fe + 4H_2O \quad (2)$$

Then, the reduced iron oxide (mainly Fe) is packed in cassettes. The cassettes will be transported to the gas stations and be mounted on PEFC vehicles. Addition of water into the cassettes would produce pure hydrogen and regenerate Fe_3O_4 according to Eq. (3). The hydrogen could be supplied directly to the PEFC on the vehicles without any purification treatment for CO.

Step 2: H_2 recovery.

$$3Fe + 4H_2O \rightarrow Fe_3O_4 + 4H_2 \quad (3)$$

The cassettes with Fe_3O_4 after water decomposition are to be exchanged for the new ones packed with Fe at residential gas stations or service stations. The used Fe_3O_4 should be recycled many times. According to Eq. (3), the theoretical amount of hydrogen being chemically stored is 4.8 wt.% of Fe. This corresponds to 4.2 kl (STP) hydrogen to be produced per 1 liter of Fe, assuming neither porosity nor pore structures in Fe. The storage capacity of hydrogen is relatively high compared to the hydrogen absorbing alloys easily obtained. The iron and iron oxide are nontoxic and quite cheap materials. These materials are stable under open air at room temperature, thus easy to be handled. Moreover, since the fuel is just water, there is no danger of explosion when the vehicles collide.

However, in order to apply the idea described above, the reduction–reoxidation kinetics and cycle life of the iron oxide have to be improved dramatically because the iron metal powders on the market are usually inactive for the production of hydrogen at <900 K due to their small surface area. Moreover, if we can get high surface area material, the decrease in the rates of reduction (Step 1) and reoxidation (Step 2) due to the sintering of Fe and Fe_3O_4 powders or pellets by repeated redox cycles cannot usually be avoided at temperatures >800 K. Under these circumstances, we explored a suitable preparation method of iron oxide and looked for favorable metal additives to the iron oxide enhancing the rates of redox of the oxide (Eqs. (1) and (2)) at low temperatures <673 K [4]. The iron oxides (initial state Fe_2O_3) prepared by co-precipitation of $Fe(OH)_3$ and foreign metal additives such as Al^{3+}, Cr^{3+}, Zr^{4+}, Ga^{3+} and V^{5+} by using urea from their aqueous solutions showed high BET surface area and high resistance against sintering after several repeated cycles. The additives enhanced both the rate of reduction (Step 1) and that of reoxidation (Step 2) at 603 and 653 K, respectively. However, the redox performances of the iron oxides with and without additives were not examined at wide range of temperature. Moreover, the effect of addition of precious metals and the synergistic effect of different metal additives have not been studied yet. Since the production of hydrogen (represents decomposition of water) on board requires the operational temperature as low as possible, one of the purposes of this work is to examine the decomposition of water at 473 K. The role of additives will also be discussed.

2. Experimental

The iron oxide samples used in this work were prepared by precipitation of $Fe(OH)_3$ from aqueous solution of $Fe(NO_3)_3$ and urea at 363 K (urea method). The precipitate $Fe(OH)_3$ was dried at 353 K for 24 h and calcined in air at 573 K for 5 h followed by further calcination at 773 K for 10 h. After these treatments, the state of iron oxide was Fe_2O_3. The iron oxide prepared by the urea method showed homogeneous fine grains (20–30 nm) and relatively high specific surface area (20 $m^2\,g^{-1}$). The Fe_2O_3 samples with foreign metal additives (M) were prepared by the same procedure by co-precipitation of $Fe(OH)_3$ and the hydroxides of foreign metal from their aqueous solutions. Usually, the nitrates of the metal additives were used as the starting materials. For addition of precious metals, their chlorides were used. For addition of Ti, V, Zr, Mo, Nb and W, $(NH_4)_2TiO(C_2O_4)_2{\cdot}2H_2O$, NH_4VO_3, $ZrCl_2O{\cdot}8H_2O$, $(NH_4)_6Mo_7O_{24}{\cdot}4H_2O$, niobium oxalate and $(NH_4)_{10}W_{12}O_{41}{\cdot}5H_2O$ were used as their salts, respectively. The amounts of added metal cations (M) were adjusted to be 3 mol% of total metal cations ($M/(Fe + M) = 0.03$).

The apparatus used for the reduction and reoxidation of the iron oxide samples was a conventional gas flow system with a fixed bed of the samples at the center of a quartz-made tubular reactor (inner diameter 8 mm). The total pressure of the gas mixture passing through the fixed bed of iron oxides was always 101 kPa. The temperature of the bed was monitored with a thermocouple touched to the outside wall of the reactor at the position of the iron oxide bed. The temperature of the iron oxide samples was controlled by an infrared radiation furnace (ULVAC, Gold Image Furnace RH-L).

The amount of iron oxide samples (powder) mounted at the bed was always adjusted to be 0.200 g as Fe or 0.286 g as Fe_2O_3. Thus, the total weight of the sample with additives was greater than 0.286 g because of the presence of additive metal oxides. The initial state of the additive oxide in the sample was assumed to be their most stable one at 773 K in air such as Al_2O_3, TiO_2, V_2O_5, Cr_2O_3, NiO, CuO, Ga_2O_3, ZrO_2, Nb_2O_5, MoO_3, Ru, Rh, PdO, AgO, CeO_2, Ta_2O_5, WO_3, Re and Pt.

The reduction of the iron oxide samples by hydrogen (Step 1) was performed with increasing the temperature of the bed linearly to the time on stream of 50:50 gas mixtures of hydrogen and argon. The total flow rate of the gas mixture was 100 ml (STP) min^{-1}. The temperature of the sample bed was changed from 563 to 823 K by a rate of 7.5 K min^{-1}. After the temperature reached to 823 K, this temperature was maintained until the consumption of hydrogen was no longer be detected.

The reoxidation of the reduced samples by water vapor (Step 2, hydrogen recovery) was followed continuously after Step 1. Before the reoxidation, the hydrogen remained in the line had been purged off by argon flow while the temperature of the bed was cooled down to room temperature. Then, water vapor (5 kPa) was co-fed with Ar (96 kPa) with total flow rate of 100 ml (STP) min^{-1}. The reoxidation of the reduced sample was started by increasing the temperature of the bed from 373 to 873 K with a rate of temperature rise of 4 K min^{-1}. After reached to 873 K, the temperature was kept at this temperature until no hydrogen formation was detected. The experimental procedures for Steps 1 and 2 described above are called as the standard experimental conditions, hereafter.

The specific surface areas of the samples were measured by the adsorption of N_2 at liquid N_2 temperature (BET method) by a surface area analyzer (Coulter SA 3100). X-ray diffraction (XRD) analysis of the samples was performed by a Rigaku RINT 2500V diffractometer using Cu Kα radiation.

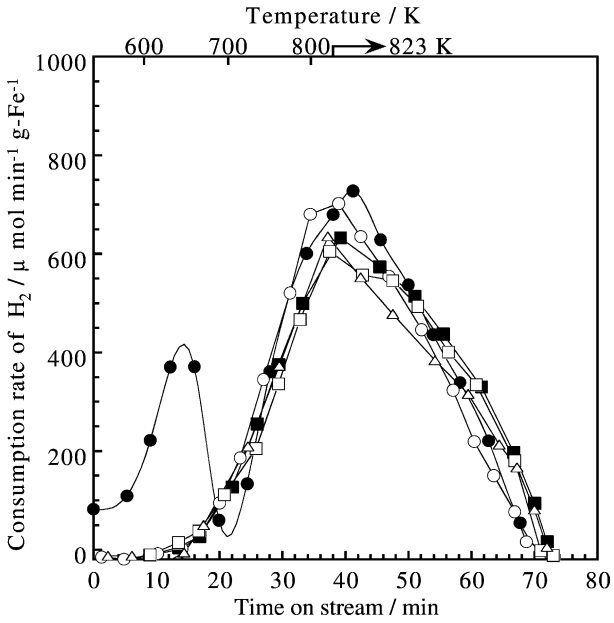

Fig. 1. Reduction of Fe-oxide (none) for five repeated cycles: consumption rate of H_2 in Step 1 vs. time on stream of H_2 (or reduction temperature). Experiment cycles: (●) first; (○) second; (□) third; (■) fourth; (△) fifth.

3. Results and discussion

3.1. Reduction and reoxidation of the iron oxide without additives

The reduction and reoxidation features of the iron oxide without additives (denoted as Fe-oxide (none)) have been studied as the reference standards for the comparison with those of the samples with foreign metal additives.

The reduction (Step 1) and reoxidation (Step 2) of Fe-oxide (none) were repeated for five cycles. The results for Steps 1 and 2 are indicated in Figs. 1 and 2, respectively. The consumption rates of hydrogen in Step 1 are plotted with time on stream for each reduction cycle in Fig. 1. The temperature of Fe-oxide bed at each time on stream is indicated in the upper horizontal axis in Fig. 1. The

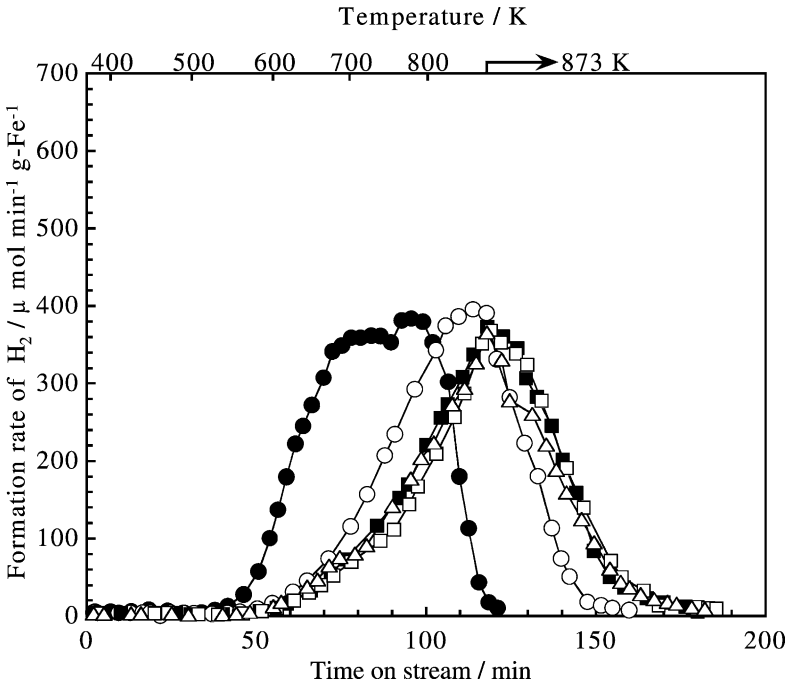

Fig. 2. Reoxidation of the reduced Fe-oxide (none) for five repeated cycles: formation rate of H_2 in Step 2 vs. time on stream of H_2O (or reduction temperature). Repeated cycles: (●) first; (○) second; (□) third; (■) fourth; (△) fifth.

consumption of hydrogen could be ascribed wholly to the reduction of Fe-oxide (none). The rapid consumption of hydrogen observed at early time on stream (or at low temperatures <650 K) for the first reduction was due to an easy reduction of Fe_2O_3 into Fe_3O_4 (Eq. (4)).

$$3Fe_2O_3 + H_2 \rightarrow 2Fe_3O_4 + H_2O \quad (4)$$

The subsequent reduction could be ascribed to the reduction of Fe_3O_4 into Fe (Eq. (2)). Since the reoxidation of Fe with H_2O (Eq. (3)) never generates Fe_2O_3, the rapid reduction of the sample by Eq. (4) did not occur from second cycle. The reduction of Fe-oxide (none) terminated almost at the same time (72 min) for all the cycles at 823 K. The rates of hydrogen formation in Step 2 for five repeated cycles are plotted in Fig. 2 as functions of time on stream. The increase in temperature with time on stream was also indicated in the upper horizontal axis. As can be seen in Fig. 2, the rate of formation of hydrogen decreased remarkably for second reoxidation, probably due to the sintering of Fe and Fe_3O_4 particles during the repeated redox cycles. However, the kinetic curves did not differ much for third to fifth reoxidation experiments.

The integrated amounts of hydrogen consumed in Step 1 for each cycle were evaluated from the areas below the curves in Fig. 1. Open bars in Fig. 3 indicate the values for each cycle. The values were normalized per gram of Fe of the sample. As described earlier, and will be indicated later, the initial state of fresh Fe-oxide (none) was Fe_2O_3. Therefore, the amount of oxygen for the fresh Fe-oxide (none) was 26.9 mmol g^{-1} of Fe. It should be noted that the amount of oxygen atoms in Fe_3O_4 was 23.9 mmol g^{-1} Fe. The amounts of hydrogen consumed in Step 1 were 10–20% less than these values. The amounts of hydrogen consumed did not change from second to fifth reduction cycle within experimental error. The integrated amounts of hydrogen produced during the reoxidation of the reduced Fe-oxide (none) in Step 2 were evaluated from the kinetic curves in Fig. 2. The amounts of hydrogen produced are also indicated in Fig. 3 by black bars for each reoxidation cycle. Almost same amount of hydrogen was produced repeatedly. The weight percent of hydrogen produced in the reoxidation step was calculated to be ca. 3.8 wt.% per Fe. The lower value than theoretical (4.8 wt.%) must be due either to incomplete reduction of the Fe-oxide (none) into Fe in Step 1 or to incomplete reoxidation of Fe to Fe_3O_4 at the preceding reoxidation (Step 2).

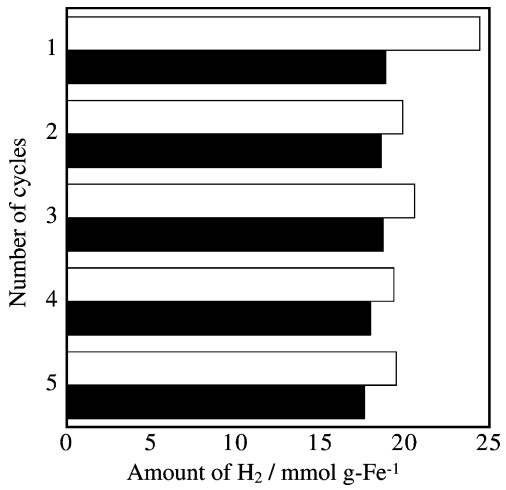

Fig. 3. Amount of H_2 consumed in Step 1 and that of produced in Step 2 for repeated redox cycles: (□) H_2 consumed in Step 1; (■) H_2 produced in Step 2.

3.2. Effects of foreign metal additives on the rate of reoxidation

For the supply of hydrogen to PEFC on board, the temperature necessary to run the reoxidation of the reduced oxide with water should be as low as possible, lower than 573 K, if possible. Therefore, in order to accelerate the rate of reoxidation of the reduced Fe-oxide samples at lower temperatures, the effects of various foreign metal additives have been investigated. The metal elements examined in this work were 26 kinds, i.e. from the small atomic number in the periodic table, Mg, Al, Ca, Sc, Ti, V, Cr, Mn, Co, Ni, Cu, Zn, Ga, Y, Zr, Nb, Mo, Ru, Rh, Pd, Ag, Ce, W, Re, Ir and Pt. The Fe-oxide sample added with metal element M is denoted as Fe-oxide (M) hereafter. Because the effects of the elements could not be categorized on the bases of the groups or series in the periodic table, we would arrange them into three groups on the basis of their peculiar effects on the reoxidation performance of Fe-oxide samples. The characteristic effects categorized are (1) the elements to be able to endow the resistance to the sample against the deactivation associated with repeated redox cycles, (2) those to worsen the reoxidation performance from the first cycle, and (3) those to enhance the rate of reoxidation at the first cycle but unable to prevent the deactivation after that. It is reasonable to expect that the additives would also affect the rate of reduction in Step 1. In fact, the kinetic curves for the first reduction showed quite complicated shapes with two maximum rates during the reduction for the Fe-oxide samples added with some foreign metal elements. However, we focused our attention to the effects of the additives on the reoxidation of the reduced samples in Step 2. The reduction of the Fe-oxides with additives for each cycle was performed under a flow of hydrogen (51 kPa) at 823 K usually in 80–120 min until no hydrogen consumption could be detected. Therefore, the kinetic curves in Step 1 for the Fe-oxides with additives will not be shown hereafter.

3.2.1. The elements able to stabilize the deactivation of Fe-oxide with repeated cycles (Al, Sc, Ti, V, Cr, Y, Zr, Mo and Ce)

The elements such as Al, Sc, Ti, V, Cr, Y, Zr, Mo and Ce belonged to this group. Among these elements, Al, Mo and Ce were the three most favorable ones for preserving the Fe-oxide from decaying its activity by repeated cycles.

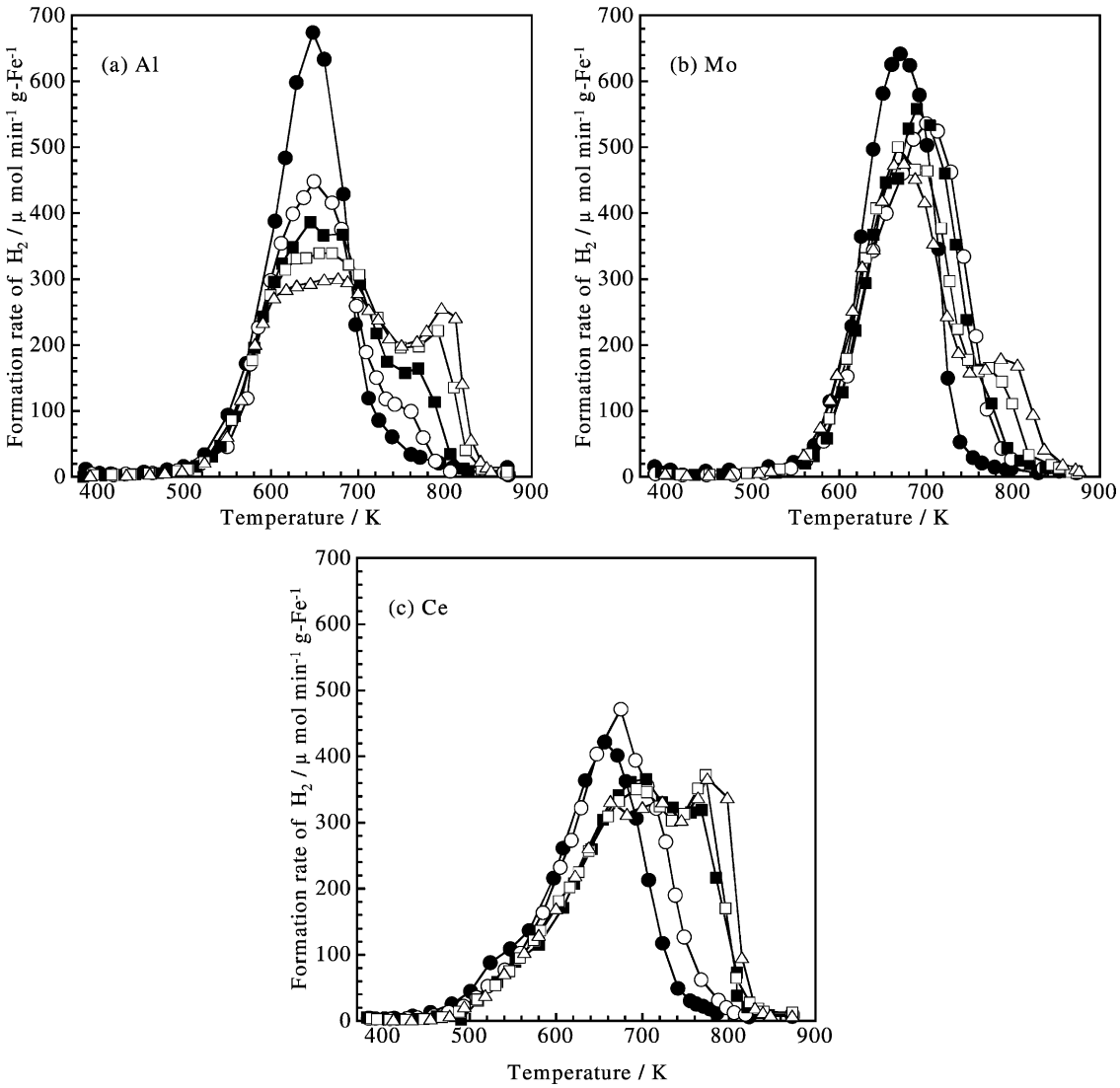

Fig. 4. Effects of additives (Al, Mo, Ce) on the formation rate of H_2 in Step 2: formation rate of H_2 vs. temperature for five repeated cycles. (a), Fe-oxide (Al); (b), Fe-oxide (Mo); (c), Fe-oxide (Ce). Repeated cycles: (●) first; (○) second; (□) third; (■) fourth; (△) fifth.

The results for the samples with Al, Mo and Ce in Step 2 are indicated in Fig. 4(a)-(c), respectively. The formation rates of hydrogen per gram Fe in the samples were plotted against temperature for repeated five cycles. As described earlier, the temperature was increased linearly from 373 to 873 K with time on stream of the gas mixture (H_2:Ar = 50:50). If one compares the kinetic curves for the first reoxidation in Figs. 2 and 4(a), it is obvious that the rate of hydrogen formation was enhanced by the addition of Al. The relative acceleration of the reaction was more obvious for the data from second cycle. The reoxidation of the reduced Fe-oxide (none) from second to fifth cycle in Fig. 2 never terminated in 125 min before the temperature reached to 873 K. However, the reoxidation completed within 125 min at <873 K for all the samples in Fig. 4 at least for five repeated cycles.

The formation rate of hydrogen showed the maximum at a temperature range 650–700 K for all the samples in Fig. 4. The second maximum appeared at 750–800 K from the second, fourth and third cycle for the Fe-oxide (Al), Fe-oxide (Mo) and Fe-oxide (Ce), respectively. The rate at the first maximum decreased, and, in contrast, that at the second maximum increased with repeated cycles.

The integrated amounts of hydrogen calculated from the areas below the curves in Fig. 4 are plotted with the number of repeated cycles in Fig. 5. The amounts of hydrogen produced until the temperature reached to 873 K at 125 min time on stream for Fe-oxide (none) in Fig. 2 were also calculated and plotted in Fig. 5. The amount of produced hydrogen decreased markedly from first to third cycle for the sample without additives. In contrast with this, the amount of the produced hydrogen did not change within experimental error for Fe-oxide (Al) and Fe-oxide (Mo). The amount of hydrogen increased with the cycles for Fe-oxide (Ce). The weight percent of the hydrogen produced per Fe in the samples at the fifth reoxidation were 3.7, 3.4, 3.3 and 2.2% for

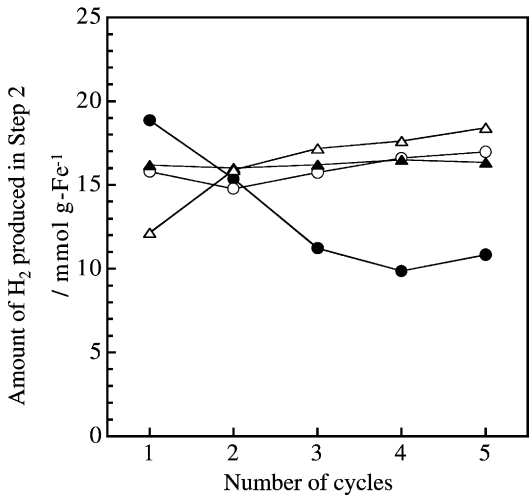

Fig. 5. Total amount of H_2 produced in Step 2 for Fe-oxide (none), Fe-oxide (Al), Fe-oxide (Mo) and Fe-oxide (Ce) at each reaction cycle: (●) Fe-oxide (none); (○) Fe-oxide (Al); (▲) Fe-oxide (Mo); (△) Fe-oxide (Ce).

Fe-oxide (Ce), Fe-oxide (Al), Fe-oxide (Mo) and Fe-oxide (none).

The reoxidation performance for Fe-oxide (Zr), Fe-oxide (Sc) and Fe-oxide (Cr) are shown in Fig. 6. The kinetic curve of the first reoxidation for Fe-oxide (Zr) (Fig. 6(a)) indicated the maximum rate of H_2 formation at 640 K. After the first redox cycle, this first maximum rate decreased sharply, and the second one at ca. 800 K increased correspondingly. The similar change in the kinetic curves was observed for Fe-oxide (Sc) in Fig. 6(b). The change was dramatic for the second and third reoxidation. The kinetic curves for Fe-oxide (Cr) in Fig. 6(c) did not show a clear peak of the rate of H_2 formation at <700 K. The rate for each cycle showed the maximum at 750–800 K.

The reoxidation of the reduced Fe-oxide (Ti), Fe-oxide (V) and Fe-oxide (Y) were also performed for five repeated cycles (not shown). The hydrogen formation terminated before the temperature reached to 873 K at 125 min for all the cycles. The kinetic curves for all these samples showed the highest rates of H_2 formation at >750 K.

The effects of alkaline earth elements (Mg, Ca) on the first reoxidation step were positive, i.e. the rate of hydrogen formation for the reduced Fe-oxide (Mg) and Fe-oxide (Ca) was markedly enhanced at a temperature range >670 K compared to Fe-oxide (none). However, total amounts of hydrogen produced in 125 min for the Fe-oxide (Mg) and Fe-oxide (Ca) decreased with repeated cycles similar to the results for Fe-oxide (none) in Fig. 5.

Fig. 7 shows the total amount of hydrogen formed at each cycle until 125 min time on stream for Fe-oxides added with Zr, Sc, Cr, Ti, V and Y. Compared to the results of Fe-oxide (none) in Fig. 5, all the samples in Fig. 7 sustained their reactivities for the decomposition of H_2O at least for five repeated cycles. Fe-oxide (Zr), Fe-oxide (Sc) and Fe-oxide (Y) are also promising samples for the use in Step 2. Relatively large difference in the amounts of H_2 produced per gram of Fe was observed among the samples in Fig. 7. This could be ascribed to how much Fe_3O_4 had been reduced to Fe in the preceding Step 1. The additives might retard the reduction or make stable compound oxides with Fe_3O_4. The study on these possibilities is quite important to elucidate the positive or negative effect of additives on the formation of H_2 in Step 2. However, since our main purpose in this work is to focus on the promising combination of additives that enhance the formation of hydrogen at low temperature, we report further the effects of other additives.

3.2.2. *The elements exerting negative effect on Step 2 (Mn, Co, Ni, Cu, Zn, Ga, Nb, W and Re)*

The effects of later first series transition metal elements (Mn, Co, Ni, Cu and Zn) were negative on the acceleration of reoxidation of the reduced samples. The results of the first and third reoxidation for the Fe-oxides added with Mn, Co, Ni, Cu and Zn are indicated in Fig. 8(a) and (b). The results of Fe-oxide (none) are also shown for comparison with those samples. It is obvious that the addition of these transition metals remarkably deteriorated the redox performances of Fe-oxides from the first cycle. Severe sintering of fine Fe-oxide particles after the reduction with hydrogen (Step 1), which was confirmed by SEM measurement described later, must be ascribed to the deteriorating effect of these additives.

The similar negative effect on the rate of reoxidation was observed for Ga, Nb, W and Re as additives. Our previous paper indicated a positive effect of Ga on the redox performance of Fe-oxide [4]. The inconsistent observation in this work can be attributed to a large discrepancy in experimental temperatures for Step 1, i.e. 603–623 K in the previous work and 823 K in this work. A severe sintering of Fe-oxide (Ga) could not be avoided probably due to the formation of solid solution or mixed crystals under the experimental conditions in the present work.

3.2.3. *Effect of noble metal elements (Ru, Rh, Pd, Ag, Ir, Pt)*

The noble metal elements such as Rh, Pd and Pt are resistant to be oxidized into their oxides in Step 2. Moreover, the compound oxides between these noble metals and Fe are not formed in general. Therefore, it is expected that the noble metals present on the surface of the particles of Fe_3O_4/Fe would activate H_2O molecules into H and OH or 2H + O. These effects must enhance the rate of reoxidation of the reduced Fe-oxide to a greater or lesser extent.

The kinetic curves of the formation rate of hydrogen at the first and third reoxidation for the Fe-oxides with the noble metals are indicated in Fig. 9(a) and (b), respectively. The addition of Rh or Ir enhanced the rate of H_2O decomposition remarkably at lower temperatures (<573 K). The enhancing effect of noble metals observed was in order of Rh > Ir >

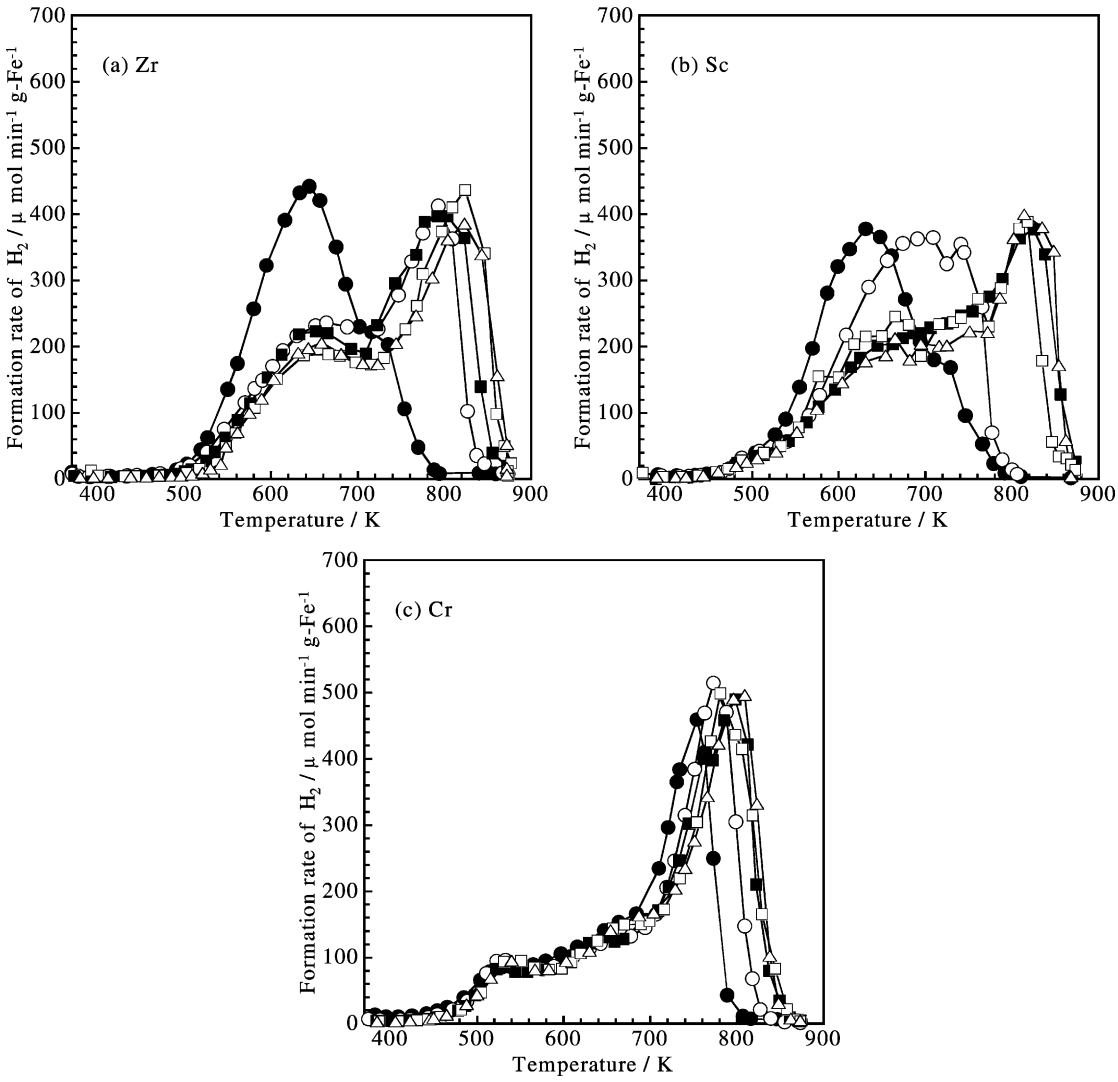

Fig. 6. Reoxidation performance of the Fe-oxide samples with Zr, Sc and Cr: Formation rate of H_2 in Step 2 vs. temperature for five repeated experiments. (a), Fe-oxide (Zr); (b), Fe-oxide (Sc); (c), Fe-oxide (Cr). Repeated cycles: (●) first; (○) second; (□) third; (■) fourth; (△) fifth.

Ag > Pd > Ru at the first reoxidation step. Pt did not show any enhancing effect.

The reoxidation of the reduced Fe-oxide (Rh) was initiated at 473 K and showed a sharp peak of hydrogen formation rate at ca. 610 K (Fig. 9(a)). However, the maximum rate as well as the total amount of hydrogen produced in 125 min dropped sharply with repeated redox cycles (Fig. 9(b)). The resemble results were also observed for the Fe-oxide with Ir, Ru, Ag, Pd or Pt, suggesting that the noble metals cannot suppress the sintering of the host iron or iron oxide.

3.2.3.1. Cooperative effect of Rh and Mo. The reoxidation performance of the reduced Fe-oxide (Mo) with repeated cycles was relatively most reproducible compared to other samples (Figs. 4–9). On the other hand, the addition of Rh enhanced the reoxidation rate most notably at low temperatures (<700 K) at the first cycle (Fig. 9(a)), but cannot protect the sintering of the host iron or iron oxide caused by repeated cycles. We speculated that the stability of Fe-oxide (Mo) might be ascribed to the resistance against the sintering by repeated redox cycles and the favorable effect of Rh be caused by the activation of H_2O molecules on the surface. Therefore, it is expected that the addition of both components may sustain the rate of reoxidation high at lower temperatures (<700 K).

The results under standard experimental conditions for the reduced Fe-oxide (Rh, Mo) are indicated in Fig. 10(a) and (b) for first and fifth reoxidation, respectively. The molar ratio of the elements was Rh:Mo:Fe = 3:3:94. For comparison, the results of Fe-oxide (Mo), Fe-oxide (Rh) and Fe-oxide (none) are also shown in Fig. 10(a) and (b). If one compares the kinetic curve of Fe-oxide (Rh, Mo) with those of Fe-oxide (Rh) or Fe-oxide (Mo) in Fig. 10(a), it is obvious that hydrogen formation by Fe-oxide (Rh, Mo) started at a low temperature (ca. 420 K), and the total amount of

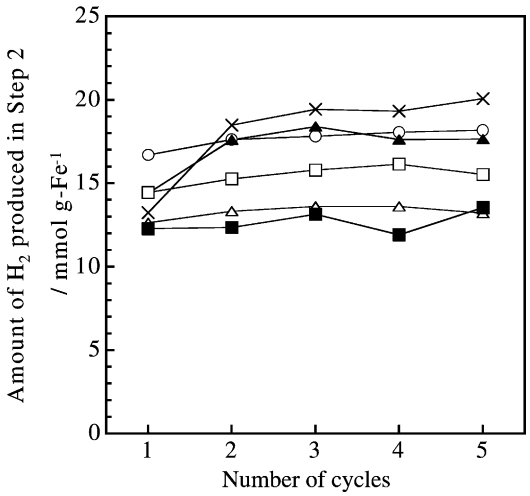

Fig. 7. Total amount of H_2 produced in Step 2 at each reaction cycle for the Fe-oxides added with Zr, Sc, Cr, Ti, V and Y. Samples: (○) Fe-oxide (Zr); (▲) Fe-oxide (Sc); (□) Fe-oxide (Cr); (△) Fe-oxide (Ti); (■) Fe-oxide (V); (×) Fe-oxide (Y).

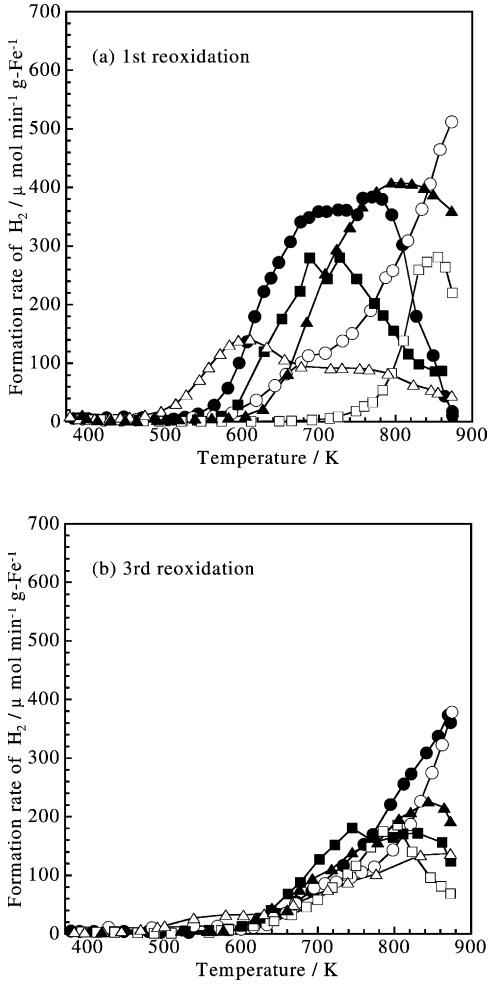

Fig. 8. Reoxidation performance of the Fe-oxides added with Mn, Co, Ni, Cu and Zn: Formation rate of H_2 in Step 2 vs. temperature for the first and third reoxidation: (●) Fe-oxide (none); (○) Fe-oxide (Mn); (■) Fe-oxide (Co); (□) Fe-oxide (Ni); (△) Fe-oxide (Cu); (▲) Fe-oxide (Zn).

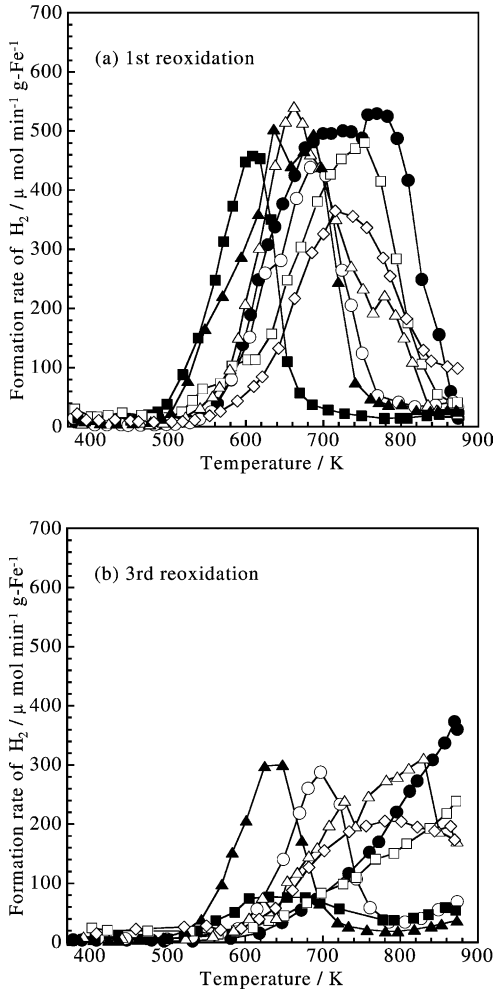

Fig. 9. Reoxidation performance of the Fe-oxides added with noble metal elements: Formation rate of H_2 in Step 2 vs. temperature for the first and third reoxidation: (●) Fe-oxide (none); (○) Fe-oxide (Ru); (■) Fe-oxide (Rh); (□) Fe-oxide (Pd); (△) Fe-oxide (Ag); (▲) Fe-oxide (Ir); (◇) Fe-oxide (Pt).

hydrogen formed was greater than those of Fe-oxide (Mo) or Fe-oxide (Rh). These observations suggest a cooperative action of Rh and Mo.

The results at fifth oxidation step for Fe-oxide (Rh, Mo) in Fig. 10(b) also indicate the acceleration of the hydrogen formation at low temperatures (<600 K) compared to those for Fe-oxide (Mo) or Fe-oxide (Rh). The temperature at the maximum rate was lower by 250 K than that for Fe-oxide (none). The temperature giving the same formation rate of hydrogen was about 30 K lower for Fe-oxide (Rh, Mo) compared to Fe-oxide (Mo). The dramatic decrease in the hydrogen formation for Fe-oxide (Rh) with cycles was avoided by co-addition of Mo. The cooperative action of the two elements was also confirmed at fifth reoxidation step.

3.2.3.2. Reoxidation at low temperatures (<573 K). The final temperatures in the experiments of Steps 1 and 2 described so far were 823 and 873 K, respectively. One of the main purposes in this work is to enhance the redox

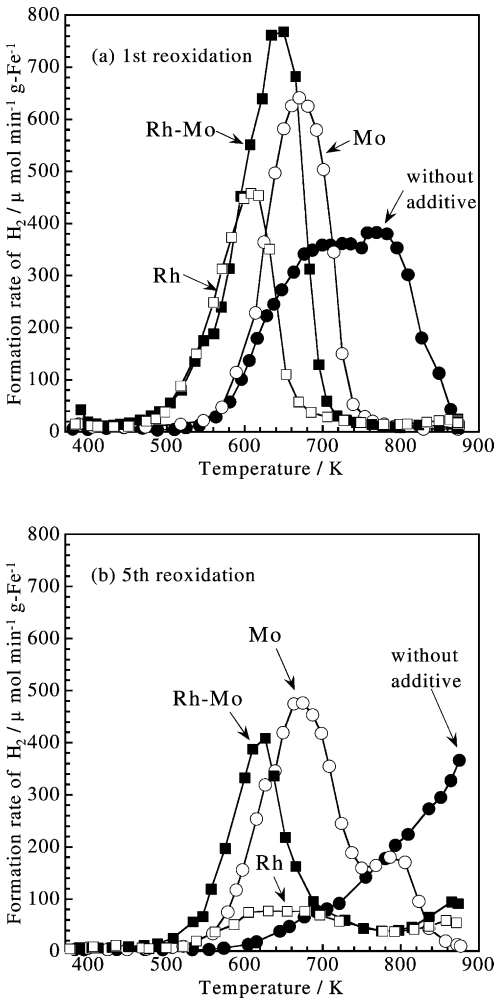

Fig. 10. Cooperative effect of Rh and Mo on the decomposition of water: Formation rate of H_2 vs. temperature for the first and fifth reoxidation: (●) Fe-oxide (none); (○) Fe-oxide (Mo); (□) Fe-oxide (Rh); (■) Fe-oxide (Rh, Mo).

performance of Fe-oxide at lower temperatures. Especially, the production of hydrogen (Step 2) at low temperatures <573 K is required for PEFC on vehicles or at homes. Moreover, the reoxidation performance of the reduced samples described so far was not observed at a fixed temperature below 873 K because the temperature was linearly increased with time. Therefore, the experiments described hereafter were performed at a fixed temperature both for Steps 1 and 2. The reduction of Fe-oxide samples (Step 1) with or without foreign metal additives was performed at 723 K for 210 min in a flow of gas mixture of H_2 and Ar (50:50, 101 kPa, flow rate 100 ml (STP) min^{-1}). The reoxidation of the reduced samples was performed at a fixed temperature (in the range of 423–573 K) until no hydrogen formation was observed.

The hydrogen formation (Step 2) for the reduced Fe-oxide samples without Rh addition was very slow at <473 K. Among the Fe-oxides co-added with Rh and other metal elements, Fe-oxide (Rh, Zr), Fe-oxide (Rh, Al), Fe-oxide (Rh, Ga) and Fe-oxide (Rh, Mo) were active in the formation of hydrogen at 473 K.

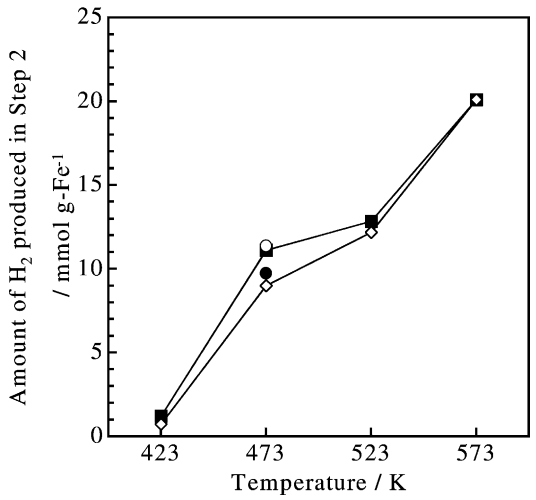

Fig. 11. The amount of H_2 produced at a fixed temperature for the Fe-oxides coadded with Rh and Zr, Mo, Al or Ga: (■) Fe-oxide (Rh, Mo); (◇) Fe-oxide (Rh, Zr); (○) Fe-oxide (Rh, Al); (●) Fe-oxide (Rh, Ga).

The amounts of hydrogen produced at a fixed temperature in Step 2 for Fe-oxide (Rh, Zr), Fe-oxide (Rh, Mo), Fe-oxide (Rh, Al) and Fe-oxide (Rh, Ga) are indicated in Fig. 11. The experiments were performed by raising temperature from 373 K to the desired temperature with a rate of 10 K min^{-1}. After reached to the desired temperature, the formation of hydrogen was measured until the reaction became no longer observable in 300 min at the fixed reaction temperature. As can be seen in Fig. 11, the amount of the formed hydrogen dropped markedly at <473 K. However, it is to be noted that the decomposition of water occurs at 473 K when Fe-oxide had been co-added with Rh and Zr, Mo, Al or Ga.

3.3. Role of additives in Fe-oxide (Rh, Mo)

The addition of Al, Cr and Zr (3 mol%) to Fe-oxide suppressed the sintering of the host oxide [1]. Consequently, the decrease in the surface area of the Fe-oxide by repeated cycles of Steps 1 and 2 was mitigated by these additives [1]. The BET surface area of Fe-oxide (none) after three redox cycles (Step 1 at 843 K, Step 2 at 573 K) decreased from 19.9 to 2.0 m^2 g^{-1}, but Fe-oxide (Mo, 3 mol%) preserved a high surface area of 14.9 m^2 g^{-1} after three cycles.

Fig. 12 indicates the SEM images of the Fe-oxide samples without and with Rh (5 mol%) and/or Mo (5 mol%) after five redox cycles (for Fe-oxide (Rh), after three cycles) under standard redox conditions (Step 1 at 823 K, Step 2 at 873 K). The images for Fe-oxide (none) and Fe-oxide (Rh) indicate a notable sintering of Fe-oxide compared to those for iron oxide (Mo) and Fe-oxide (Rh, Mo). These observations suggest that the addition of Mo mitigates the coagulation of iron oxide particles.

Fig. 13 indicates the XRD spectra for Fe-oxide (Mo) after first and fifth reoxidation as well as for Fe-oxide (none) after fifth reoxidation. The spectrum for a Fe_3O_4 obtained

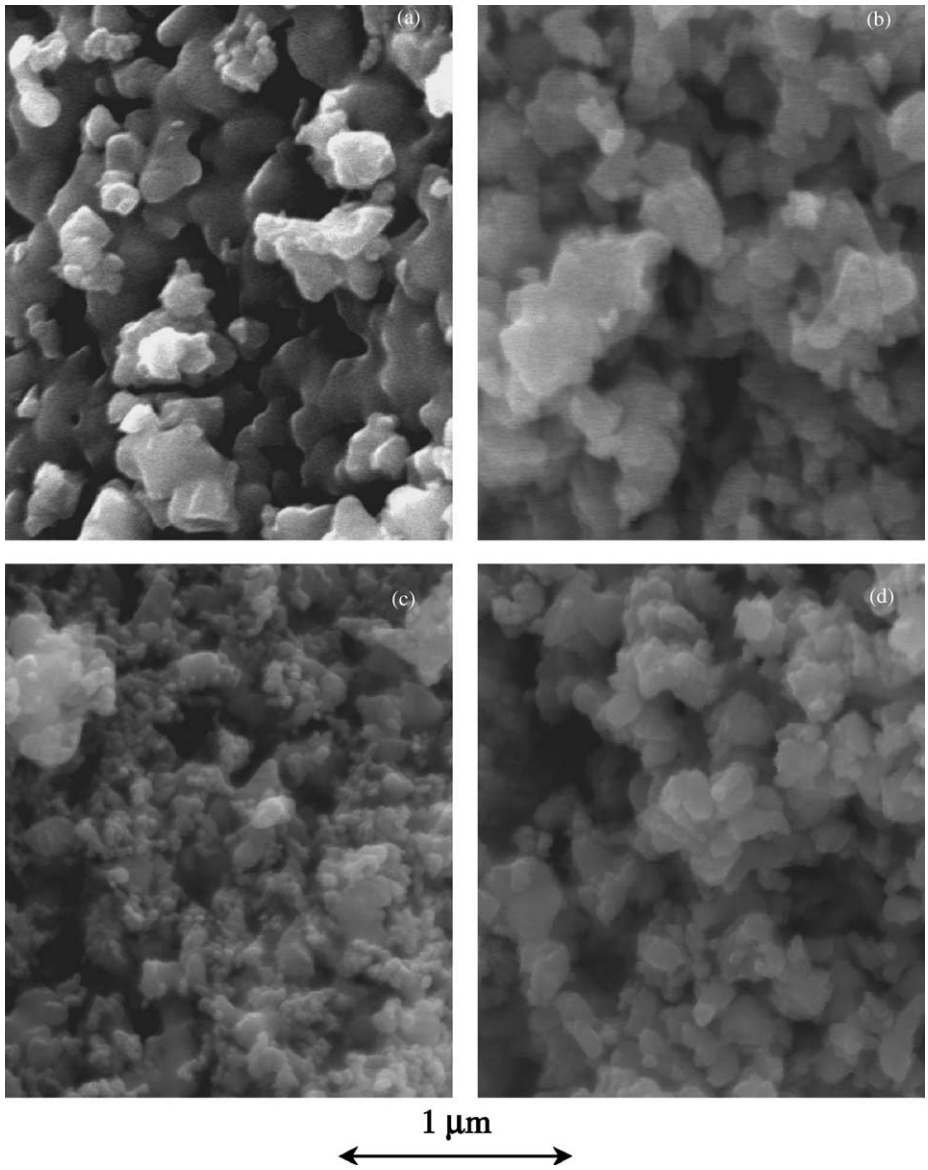

Fig. 12. SEM images of (a) Fe-oxide (none) after fifth reoxidation, (b) Fe-oxide (Rh) after third reoxidation, (c) Fe-oxide (Mo) after fifth reoxidation, and (d) Fe-oxide (Rh, Mo) after fifth reoxidation.

from Wako Pure Chem. Co. is also indicated as a reference in Fig. 13. The content of Mo in the Fe-oxide (Mo) sample was increased to 5 or 10 mol% in order to check the presence of an isolated molybdenum oxide phase such as MoO_3 and MoO_2. The redox of the Fe-oxide (none) and Fe-oxide (Mo) had been repeated under standard reaction conditions (Step 1 at 823 K, Step 2 at 873 K). All the spectra in Fig. 13 gave only the diffraction peaks due to magnetite (Fe_3O_4). The diffraction peak due to Rh metal was observed for the sample added with Rh. For the Fe-oxide (none) after fifth reoxidation, the peak due to the unreacted Fe metal was observed, indicating that the complete reoxidation was not possible. The spectrum for Fe-oxide (Mo 10 mol%) did not show any peaks ascribed to molybdenum oxide phases. These observations suggest that the added Mo cations would have been taken into the host Fe-oxide, generating a Mo-Fe compound oxide, ferrite, at the final stage of Step 2. The ferrite gives the same diffraction patterns as those of Fe_3O_4. The formation of the ferrite might prevent the host Fe-oxide particles from severe sintering.

X-ray absorption near edge structure (XANES) and extended X-ray absorption fine structure (EXAFS) studies on the Fe-oxide (Mo 5 mol%) samples after reduction (Step 1) and reoxidation (Step 2) also suggested the formation of the ferrite ($Mo_xFe_{3-x}O_4$) [5]. The valence state of molybdenum changed from Mo(IV) to Mo(III) in the reduction (Step 1) and Mo(III) to Mo(IV) in the reoxidation (Step 2). We speculate that the redox between Mo(III) and Mo(IV) might enhance the redox between Fe_3O_4 and Fe. Detailed studies on the state of molybdenum by XANES and EXAFS spectroscopies will be reported in the near future [5].

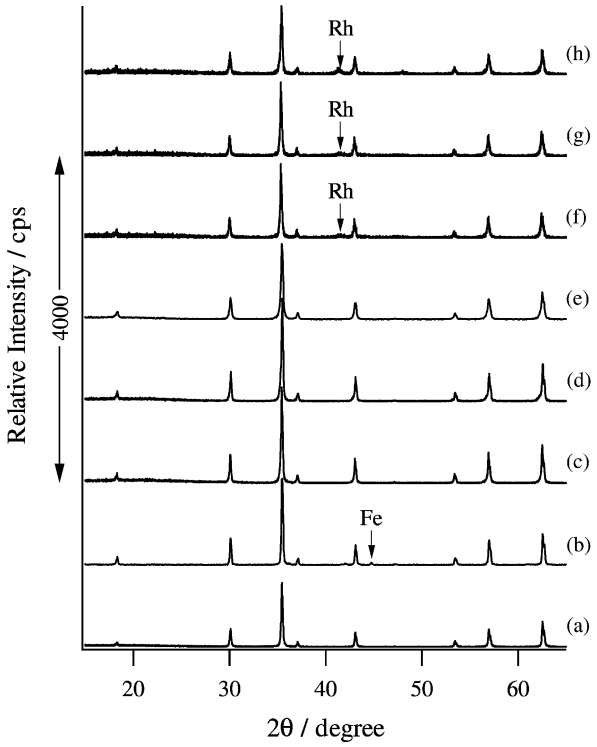

Fig. 13. XRD spectra of the Fe-oxides without and with Mo and/or Rh. (a) Fe_3O_4 (Wako Pure Chem. Co.) as reference; (b) Fe-oxide (none) after five cycles; (c) Fe-oxide (Mo 5 mol%) after one cycle; (d) Fe-oxide (Mo 5 mol%) after five cycles; (e) Fe-oxide (Mo 10 mol%) after one cycle (intensity 0.5 times); (f) Fe-oxide (Rh 5 mol%) after five cycles (intensity four times); (g) Fe-oxide (Rh 5 mol%, Mo 5 mol%) after one cycle (intensity four times); and (h) Fe-oxide (Rh 5 mol%, Mo 5 mol%) after five cycles (intensity four times).

The XRD spectrum for the Fe-oxide (none) after reduction (Step 1) indicated only the formation of α-Fe. The reoxidation (Step 2) at the first cycle gave only the spectrum due to Fe_3O_4. The measurements of XRD spectra after the reduction for the samples added with Mo, Zr, Al, Ga and Cr were not successful because the samples had been oxidized quickly in air at room temperature.

The XRD spectra for Fe-oxide (Rh 5 mol%, Mo 5 mol%) after first and fifth reoxidation indicated very resemble diffraction patterns to those of Fe-oxide (Mo) in Fig. 13 except for the peak due to Rh metal in the former case, suggesting that Rh would not influence the structure of Fe-oxide (Mo). The Rh metal on the surface of $Mo_xFe_{3-x}O_4$ must catalyze the dissociation of H_2O in Step 2, accelerating the reoxidation of bulk Fe metal into Fe_3O_4 at a low temperature, 473 K.

References

[1] K. Otsuka, C. Yamada, T. Kaburagi, S. Takenaka, in: R.D. Venter, T.K. Bose, N. Veziroglu (Eds.), Proceedings of the 14th World Hydrogen Energy Conference, Montreal, Canada, Session Al.9–Storage and Material Systems I, CD-ROM, 2002.
[2] P.B. Tarman, D.V. Punwani, Hydrogen production by the steam-iron process, Proc. Intersoc. Energy Convers. Eng. Cont. 11 (1976) 286–293.
[3] P.B. Tarman, R. Biljetina, Coal Process Technol. 5 (1979) 114–116.
[4] K. Otsuka, C. Yamada, T. Kaburagi, S. Takenaka, Int. J. Hydrogen Energy 28 (2003) 335–342.
[5] S. Takenaka, T. Kaburagi, K. Otsuka, J. Catal., submitted for publication.